



RESEARCH ARTICLE

OXYGEN ENHANCED MICROGRAVITY ETHANE FLAMES

*Pramod Bhatia

Department of Mechanical Engineering, The NorthCap University, Gurgaon 122017

ARTICLE INFO

Article History:

Received 24th March, 2016
Received in revised form
06th April, 2016
Accepted 21st May, 2016
Published online 30th June, 2016

ABSTRACT

Ethane flames, for four different fuel compositions and two flame configurations were simulated on earth and in zero-gravity. Temperature contours were compared with the experimental photographs. As expected, the flame temperature increases with oxygen enhancement for all flames. Gravity and oxygen variation did not have any significant effect on flame length for inverse flames.

Key words:

Ethane, Flames,
Zero-gravity,
Oxygen-enhancement,
One-step chemistry.

Copyright©2016, Pramod Bhatia. This is an open access article distributed under the Creative Commons Attribution License, which permits unrestricted use, distribution, and reproduction in any medium, provided the original work is properly cited.

Citation: Pramod Bhatia, 2016. "Oxygen enhanced microgravity ethane flames", *International Journal of Current Research*, 8, (06), 33322-33326.

INTRODUCTION

There has been increasing interest in diffusion and inverse-diffusion flames by scientific community. These situations are possible on earth and in space (Baukal, 1998). Increase in oxygen and change in gravity can significantly affect flame behavior. The temperatures of some hydrocarbons increase by about 38 percent or more in the presence of oxygen compared (Table 1). The buoyant flames have been reported to be shorter than buoyant flames (Sunderland *et al.*, 1999).

OBJECTIVES

The aim of the present work is to study flame characteristics under following situations:

- Zero-gravity and earth.
- Varying oxygen in the oxidizer.
- Inverse and normal configurations.

One-step version of the axi-symmetric computational tool developed by Katta *et al.* (1994; Roquemore *et al.*, 2000) was used.

*Corresponding author: Pramod Bhatia,
Department of Mechanical Engineering, The NorthCap University,
Gurgaon 122017.

Comparisons between computational results and experimental data (Sunderland *et al.*, 2004) are shown in this paper. In the present study, ethane was used as the fuel. Zero gravity and earth-gravity calculations were completed for inverse-diffusion flames. Table 1 summarizes the eleven steady-state computations. Transient computations were also completed for CASE 1.

Computational Modeling

The computational code was developed by Katta *et al.* (1994; Roquemore *et al.*, 2000). A round burner of 5.5 mm diameter, ambient pressure of 0.98 bars and ambient temperature of 298 K have been assumed in the present study. The five species considered in the calculations are: Oxygen, Nitrogen, H₂O, Carbon-dioxide and Ethane. The geometry of the computational domain is shown in Figure 1.

The computational domain extends 25 mm X 100 mm in the radial and axial directions. A uniform 141 X 401 grid has been used in this study. The coflow velocity is assumed to be one-tenth of the jet-velocity. Boundary conditions are summarized in Table 1. Heat of formation, specific-heat, viscosity, thermal conductivity and mass diffusivity are assumed to be temperature dependent (Roquemore *et al.*, 2000).

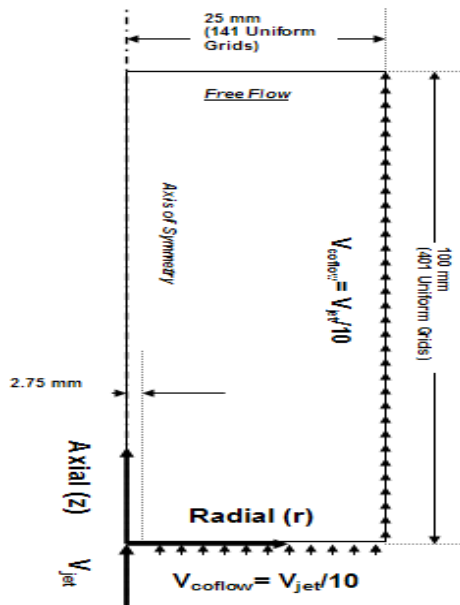


Figure 1. Computational Domain

RESULTS AND DISCUSSION

Summary of all the cases is shown in Table 1. Centerline axial velocity profile as a function of burner till is shown in Figure 2. The figure shows that volumetric expansion caused by the combustion heat release increases the upstream axial velocity. Beyond the flame tip the axial velocities increase with distance for the 1-g cases (Figures 2 & 5.1-8), whereas it decreases for the 0-g (Figure 2 & 5.9-11) cases as expected. These effects are expected because of the high product temperatures leading to lower density and resultant buoyant accelerations in the 1-g cases, in contrast to the deceleration caused by shear forces for the 0-g cases. These effects decrease with downstream distance and the axial velocities start approaching uniform profiles. With identical oxygen, no significant differences in maximum flame temperatures and maximum temperature based flame lengths were observed between 1-g and 0-g inverse-diffusion flames.

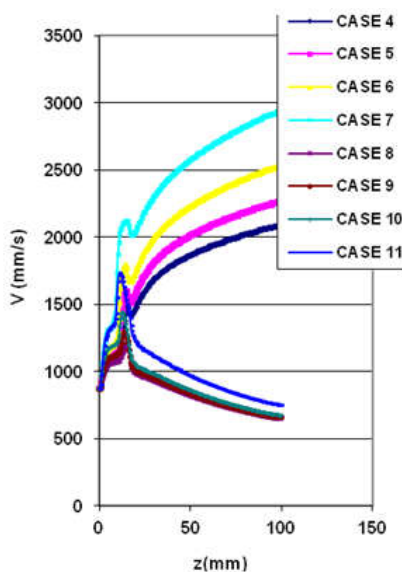


Figure 2. Axial-Velocity Vs. z (r=0)

The temperature (Figure 3) and fuel mass fraction (Figure 4) along the axial direction (at $r=0$) show similar values for the zero-gravity and earth-gravity inverse-diffusion flames. The flame temperatures rise with increase in the inlet oxygen content. The centerline C_2H_6 mass fraction values increase in a similar manner for all inverse diffusion flames and decrease monotonically for all normal diffusion flames (Figure 4).

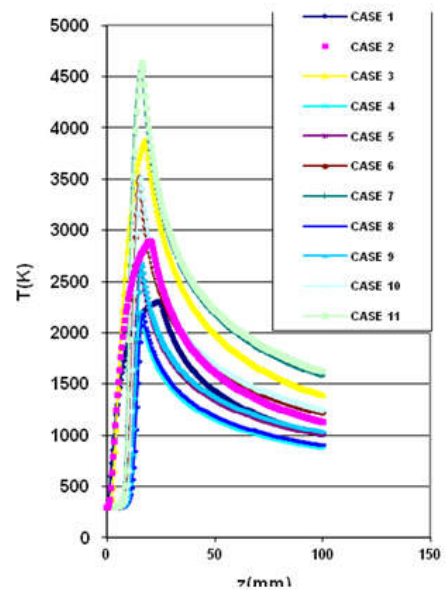
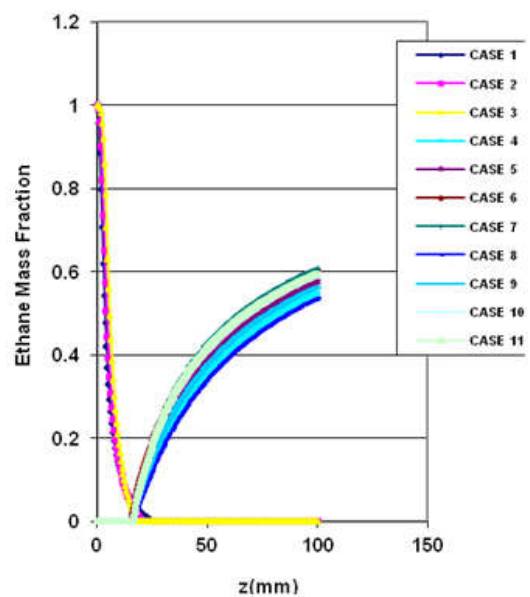


Figure 3. Temperature Vs. z (at r=0)

Figure 4. C_2H_4 Mass Fraction Vs. z (r=0)

Figures 5.1 to 5.11 show flame photographs from Ref. (Sunderland *et al.*, 2004) and temperature contours and velocity vectors from the present computations. Given that there are differences in the quantities being compared and that the boundary conditions are different, the comparisons can only be qualitative. Final converged unsteady computations conducted for CASE 1 show no significant differences with the results obtained from its steady computations.

Table 1. Summary of computed cases

	Gravity	Diffusion	Inlet O ₂ Mole Fraction	Jet Velocity (mm/s)	Flame Length (mm) Based on T _{max}	T _{max} (K)	T (K) Adiabatic Global Calculations 5 Species	T (K) Adiabatic Cea Calculations 2000 Species
CASE 1	1-g	Normal	0.21	24	24	2300	2382	2250
CASE 2	1-g	Normal	0.3	74	20	2900	2977	2553
CASE 3	1-g	Normal	0.5	124	17.7	3870	3981	2839
CASE 4	1-g	Inverse	0.21	866	16	2190	2382	2250
CASE 5	1-g	Inverse	0.3	866	15.2	2690	2977	2553
CASE 6	1-g	Inverse	0.5	866	15.2	3510	3981	2839
CASE 7	1-g	Inverse	1.0	866	15.8	4640	5491	3082
CASE 8	0-g	Inverse	0.21	866	15.3	2180	2382	2250
CASE 9	0-g	Inverse	0.3	866	15.8	2680	2977	2553
CASE10	0-g	Inverse	0.5	866	15.8	3510	3981	2839
CASE11	0-g	Inverse	1.0	866	15.3	4630	5491	3082

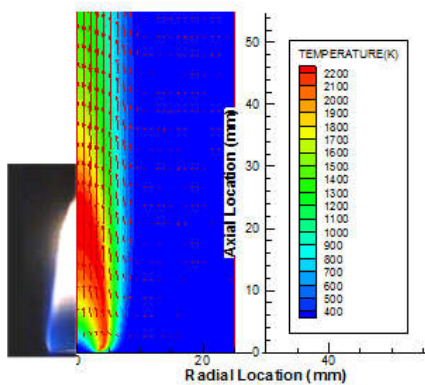


Figure 5.1 : Case 1

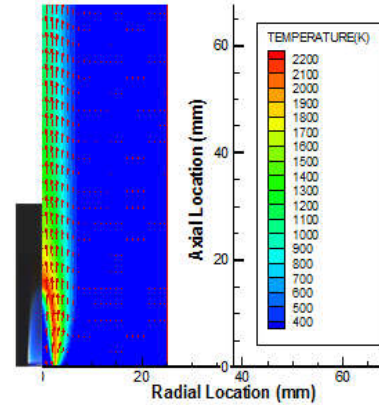


Figure 5.4 : Case 4

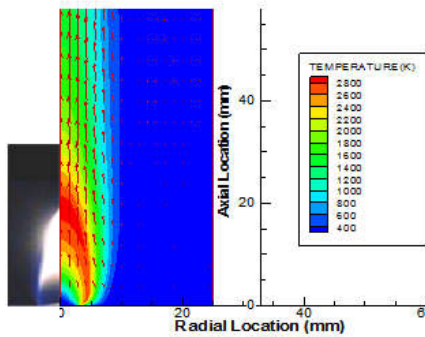


Figure 5.2 : Case 2

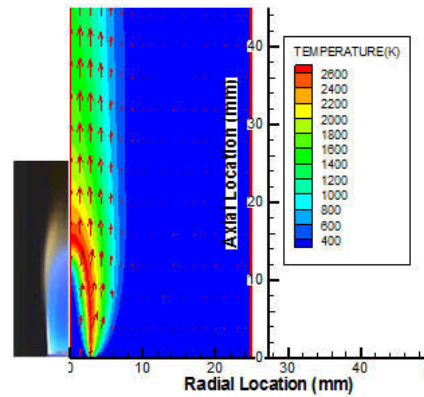


Figure 5.5 : Case 5

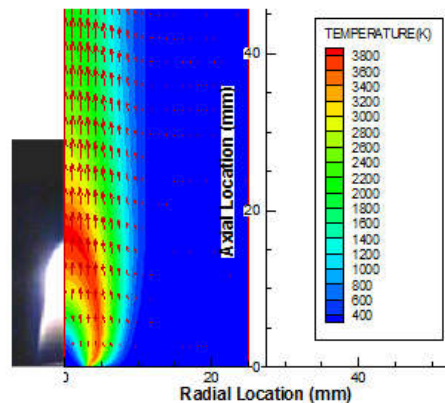


Figure 5.3. Case 3

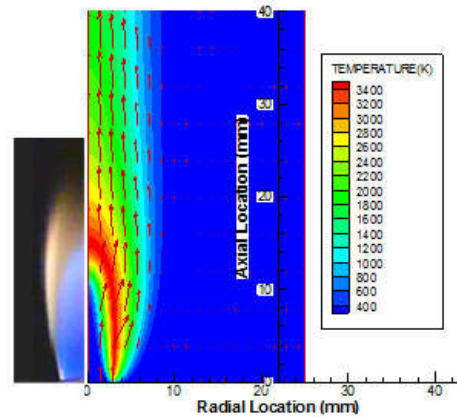


Figure 5.6. Case 6

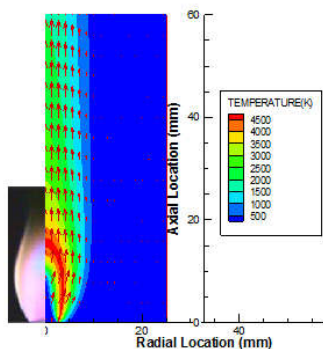


Figure 5.7 : Case 7

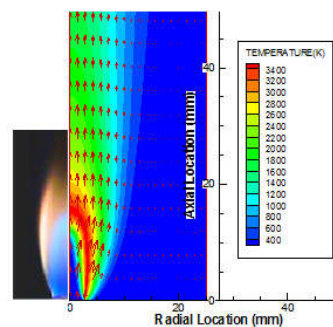


Figure 5.10 : Case 10

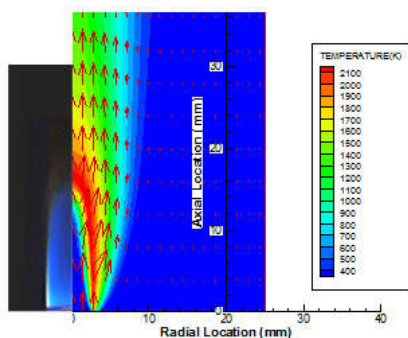


Figure 5.8 : Case 8

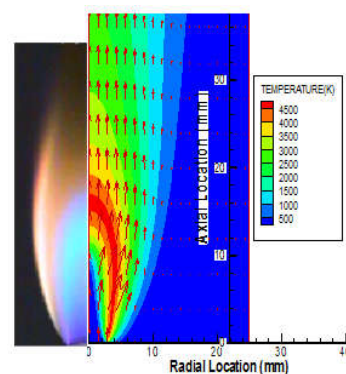


Figure 5.11 : Case 11

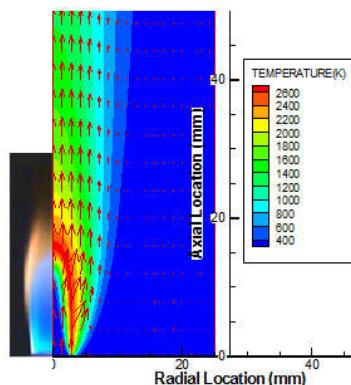


Figure 5.9: Case 9

Figure 5.1 – 11 Comparisons between Computational and Experimental Results.
(Left: Experimental Results [5]; Right: Computational Results: Temperature and velocity profiles)

Figures 5.1 to 5.11 show remarkable qualitative similarities between experimental and computational results. These trends are encouraging but more work is needed as discussed in the following. A comparison of the adiabatic equilibrium temperatures for the different cases presented in Table 1 with the maximum temperatures computed by the present global chemistry model and approximate thermo-physical property assumptions reveals significant differences with increases in oxygen concentrations. The adiabatic temperatures are lower than the calculated temperatures. This is because the current assumption of specific heats and the limitations of global kinetic steps which appear to prevent high temperature dissociation which may be prevalent in oxygen enriched flames.

Experimental measurements of temperature distributions and improved computations with detailed chemistry and radiation models are necessary to resolve these issues.

Conclusion

Computations were performed for ethane fueled laminar flames. Effects of oxygen variation and gravity change were studied on normal and inverse flames. Qualitative comparisons between experimental photographs and computational results were performed (5). The major findings were:

- As expected, increase in oxygen increases the temperature of fame as well as the gas velocities.

- For inverse-diffusion flames, gravity has relatively small influences on the flame temperature and fuel mass fraction distributions.
- The axial velocities increase significantly before the flame tip for the normal and zero gravity flames as a result of expansion caused by heat release. Beyond the flame tip the velocities increase for the 1-g flames whereas they decrease for 0-g flames.
- In case of inverse diffusion flames, the gravity-variation and oxygen-enhancement had no significant effect on the flame length (based on maximum temperature).
- Comparisons of maximum temperatures based on present thermo-physical properties and global kinetic rates with adiabatic equilibrium temperatures show that the computations may be overestimating the non-equilibrium effects by underestimating the rates of dissociation reactions. Temperature measurements and detailed chemistry and thermo-physical property calculations are necessary to address these issues.

REFERENCES

- Baukal, C.E. 1998. in: C.E. Baukal (Ed.), Oxygen-Enhanced Combustion, CRC Press, Boca Raton, pp. 2-42.
- Katta, V. R., Goss, L. P. and Roquemore, W. M. 1994. "Effect of nonunity Lewis number and finite-rate chemistry on the dynamics of a hydrogen-air jet diffusion flame" Combustion and Flame, Vol. 96, pp. 60-74.
- Roquemore, W. M. and Katta, V. R. 2000. Role of Flow Visualization in the development of UNICORN, Journal of Visualization, Vol 3/4, Pg 257-272.
- Sunderland, P. B., Krishnan, S. S. and Gore, J. P. 2004. Effects of oxygen enhancement and gravity on normal and inverse laminar jet diffusion flames, Combustion and Flame, Volume 136, Issues 1-2, January, Pages 254-256.
- Sunderland, P.B., Mendelson, B.J., Yuan, Z.G. and Urban, D.L. 1999. "Shapes of Buoyant and Nonbuoyant Laminar Jet Diffusion Flames," Combust. Flame, Vol. 116, pp. 376-385.
